Genesis. Author manuscript; available in PMC 2014 October 29.

Published in final edited form as:
Genesis. 2011 April ; 49(4): 278–294. doi:10.1002/dvg.20707.

Molecular analysis of neurogenic placode development in a basal ray-finned fish

Melinda S. Modrell[1], **David Buckley**[2], and **Clare V.H. Baker**[1,*]

[1]Department of Physiology, Development and Neuroscience, University of Cambridge, United Kingdom

[2]Department Biodiversidad y Biología Evolutiva, Museo Nacional de Ciencias Naturales, CSIC, Madrid, Spain

Abstract

Neurogenic placodes are transient, thickened patches of embryonic vertebrate head ectoderm that give rise to the paired peripheral sense organs and most neurons in cranial sensory ganglia. We present the first analysis of gene expression during neurogenic placode development in a basal actinopterygian (ray-finned fish), the North American paddlefish (*Polyodon spathula*). *Pax3* expression in the profundal placode confirms its homology with the ophthalmic trigeminal placode of amniotes. We report the conservation of expression of *Pax2* and *Pax8* in the otic and/or epibranchial placodes, *Phox2b* in epibranchial placode-derived neurons, *Sox3* during epibranchial and lateral line placode development, and *NeuroD* in developing cranial sensory ganglia. We identify *Sox*3 as a novel marker for developing fields of electrosensory ampullary organs and for ampullary organs themselves. *Sox3* is also the first molecular marker for actinopterygian ampullary organs. This is consistent with, though does not prove, a lateral line placode origin for actinopterygian ampullary organs.

Keywords

paddlefish; sensory ganglia; otic; epibranchial; electroreceptors; lateral line

INTRODUCTION

Vertebrate cranial placodes are paired patches of thickened ectoderm found in the embryonic head that give rise to the paired peripheral sense organs (olfactory epithelia, inner ears and lateral line system), most neurons in cranial sensory ganglia, plus the adenohypophysis (anterior pituitary gland) and eye lenses (reviewed in Baker and Bronner-Fraser, 2001; Schlosser, 2006; Schlosser, 2010). All cranial placodes originate from a common “pre-placodal region” or “pan-placodal primordium” (Schlosser, 2010; Streit, 2007), i.e., a crescent of ectoderm around the anterior neural plate characterized by expression of members of the Eya, Six1/2, and Six4/5 families of transcription factors or co-

*Address for Correspondence: Clare V. H. Baker, Department of Physiology, Development and Neuroscience, University of Cambridge, Anatomy Building, Downing Street, Cambridge CB2 3DY, United Kingdom, Tel +44 (0) 1223 333789, Fax +44 (0) 1223 333840, cvhb1@cam.ac.uk.

Europe PMC Funders Author Manuscripts

factors, whose expression is maintained in all cranial placodes and their derivatives (reviewed by Schlosser, 2010; Streit, 2007). An explosion of molecular information and functional experiments over the past decade has greatly increased our understanding of the mechanisms underlying the induction of the preplacodal region itself, its subsequent regionalization and the formation of individual placodes and their derivatives (reviewed by Ladher *et al.*, 2010; Schlosser, 2010; Streit, 2007).

Most modern studies of neurogenic placode development have focused on a handful of osteichthyan (bony fish) models, notably tetrapods (two amniotes, i.e., mouse and chick, plus the anuran amphibian *Xenopus*) and teleost fish (mainly zebrafish). Tetrapods and teleosts are members, respectively, of the two sister groups of bony fish: sarcopterygians (lobe-finned fish) and actinopterygians (ray-finned fish) (see Fig. 1a). In order to understand the development and evolution of any process or trait across vertebrates, it is important to include as many phylogenetically informative taxa as possible. Although teleosts are by far the most speciose actinopterygian group, there are also four extant non-teleost actinopterygian taxa: polypterids (bichirs), which are accepted as the most basal actinopterygian group (see e.g. Hurley *et al.*, 2007), chondrosteans (sturgeons and paddlefish), lepisosteids (gars) and amiids (bowfin). The precise phylogenetic relationship of chondrosteans, lepisosteids, amiids and teleosts is still debated (see Hurley *et al.*, 2007; Inoue *et al.*, 2003; Venkatesh *et al.*, 2001). Cladistic analysis of morphological data from extant and fossil taxa, as well as Bayesian and maximum likelihood analysis of nuclear molecular data, provide strong statistical support for chondrosteans (sturgeons and paddlefish) as the sister group to a monophyletic neopterygian clade comprising lepisosteans, amiids and teleosts (Hurley *et al.*, 2007). Regardless of their precise phylogenetic placement, all non-teleost actinopterygians occupy a position of great importance in vertebrate phylogeny. Furthermore, comparative developmental studies in basal actinopterygians do not have to take into account the extra round of whole-genome duplication that occurred in the teleost lineage (see e.g. Hurley *et al.*, 2007).

Embryos of the chondrostean fish *Polyodon spathula* (North American paddlefish) can be obtained in large numbers from commercial fisheries and are relatively easy to manipulate (see e.g. Davis *et al.*, 2004; Davis *et al.*, 2007). The paddlefish is also a particularly interesting actinopterygian model for understanding the development and evolution of the peripheral sensory nervous system, since chondrosteans (like polypterids, but unlike lepisosteids, amiids and teleosts) have retained the ancestral electrosensory division of the lateral line system (Bullock, 1982; Bullock *et al.*, 1983), which enables the passive detection of weak electric fields in water and is used in prey or predator detection and orientation. Electrosensory hair cells, which are innervated by lateral line placode-derived neurons, are collected together with supporting cells in “ampullary organs” connected to the surface by canals filled with electrically conductive jelly (reviewed in Jørgensen, 2005). Shark electrosensory hair cells were recently proposed, on the basis of gene expression alone, to be derived from the neural crest (Freitas *et al.*, 2006). However, in a tetrapod, the axolotl *Ambystoma mexicanu*m (a urodele amphibian), fate-mapping and ablation studies showed that ampullary organs and the electrosensory hair cells within them arise from lateral line placodes (Northcutt *et al.*, 1995). Lateral line placodes (of which primitively there are six pairs: three pre-otic and three post-otic; Northcutt, 1997) give rise to lateral line primordia

that elongate or migrate over the head and trunk and deposit characteristic lines of sense organs called neuromasts, which contain mechanosensory hair cells innervated (like electrosensory hair cells) by lateral line placode-derived neurons (reviewed in Baker *et al.*, 2008; Ghysen and Dambly-Chaudière, 2007; Ma and Raible, 2009; Schlosser, 2002). Fields of ampullary organs develop on either side of the cranial lines of mechanosensory lateral line neuromasts (reviewed in Baker *et al.*, 2008; Schlosser, 2002; Schlosser, 2010). The paddlefish is a superb model for ampullary organ development, as it has more ampullary organs than any other vertebrate species: indeed the characteristic rostrum ("paddle") of the paddlefish, an extension of the cranium, is covered in ampullary organs and used as an electrosensory "antenna" for feeding (Wilkens *et al.*, 1997; Wojtenek *et al.*, 2001).

Here, we confirm the conservation of expression of a range of known neurogenic placode markers in paddlefish, including *Pax3* specifically in the profundal placode and ganglion (thus confirming the homology of the anamniote profundal placode with the amniote ophthalmic trigeminal placode), *Pax2/5/8* family members in the otic and/or epibranchial placodes, *Phox2b* in epibranchial placode-derived neurons, and *Sox3* during otic, epibranchial and lateral line placode development. *Sox3* is not only expressed in all lateral line placodes and maintained in elongating and migrating lateral line primordia, as in *Xenopus* (Schlosser and Ahrens, 2004); it is also expressed broadly in developing ampullary organ fields and in ampullary organs themselves. Thus, *Sox3* is a novel molecular marker for developing vertebrate ampullary organs, and also the first published molecular marker for actinopterygian ampullary organs. This result is compatible with (though of course does not prove) a lateral line placode origin for ampullary organs in actinopterygian fish.

RESULTS

Isolation of neurogenic placode and placode-derived neuron markers in paddlefish

Using a degenerate PCR-based approach, we cloned cDNA fragments of seven transcription factors predicted to be expressed in neurogenic placodes and/or neurogenic placode-derived neurons, in a basal actinopterygian (ray-finned fish), *Polyodon spathula* (the North American paddlefish). We cloned *Pax3* as a putative profundal placode marker; *Pax2, Pax5* and *Pax8* as putative otic and/or epibranchial placode markers; *Phox2b* as a putative epibranchial placode-derived neuron marker; *Sox3* as a putative lateral line placode marker; and *NeuroD* as a putative pan-neuronal marker. The various PCR products were sequenced and their identity determined by BLAST (NCBI) searches, followed by phylogenetic analysis (Fig. 1; see Materials and Methods for details).

We performed whole-mount *in situ* hybridization on paddlefish embryos at different developmental stages to determine the spatiotemporal expression of these transcripts during neurogenic placode and cranial sensory ganglion development. Our analyses extended from stage 24 (end of neurulation) to stage 46 (the start of feeding) (Ballard and Needham, 1964; Bemis and Grande, 1992). Briefly, stage 24 embryos have nearly completed neurulation and the primary divisions of the brain into forebrain, midbrain, and hindbrain are evident. By stage 26, the olfactory placode, eyes and otic vesicles can be discerned, as well as the lateral spreading of the pharyngeal arches over the yolk as they begin to fold ventrally during the process of "head lifting", which results in the separation and rostral growth of the head from

the yolk. The process of head formation continues through stages 32-33. At stage 36, hatching occurs, resulting in a yolk-sac larva. Stages 37 through 46 primarily involve the continued development and diversification of sensory and feeding systems.

Pax3 is a conserved marker for the profundal placode and ganglion

We examined expression of the paired-domain homeodomain transcription factor *Pax3* in paddlefish as a putative marker for the profundal placode, which forms somatosensory neurons in the profundal ganglion. It has been proposed that the separate profundal and trigeminal ganglia found in many anamniotes (e.g. sharks, basal actinopterygians, urodele amphibians) are, respectively, homologous to the ophthalmic and maxillomandibular lobes of the fused amniote trigeminal ganglion, whose neurons arise, respectively, from the ophthalmic trigeminal placode and the maxillomandibular trigeminal placode (plus the neural crest) (see O'Neill *et al.*, 2007; Schlosser, 2006; Schlosser and Northcutt, 2000; Xu *et al.*, 2008).

At stage 26, *Pax3* expression was seen in the developing somites and presomitic region, dorsal neural tube and migrating cranial neural crest cells (Fig. 2a,b). *Pax3* transcripts were also observed in the profundal placode as two bilateral patches of ectoderm, on either side of the developing midbrain (Fig. 2a,b; compare with location of profundal and trigeminal placode-derived neurons in Fig. 7b,c). The *Pax3*-positive placodal cells appeared to be loosely associated at this stage of development (Fig. 2b), but by stage 29, they had begun to condense into a tight (though still superficial) cluster (Fig. 2c,d). By this stage, neural crest cells no longer expressed *Pax3*, although expression was still observed in the dorsal neural tube and, weakly, in the olfactory pits (Fig. 2c,d). By stage 32, the *Pax3*-positive profundal cells had migrated into the mesenchyme towards the final position of the profundal ganglion as seen in whole-mount (Fig. 2e,f; compare with Fig. 7e,h) and in transverse sections (Fig. 2g,h). After stage 32, *Pax3* was downregulated in the profundal ganglion (Fig. 2i,j) and could only be observed in the central nervous system thereafter.

Pax2 is a conserved marker for the otic and epibranchial placodes

The Pax2/5/8 family of paired domain transcription factors plays varied and important roles during embryonic development, including in the formation of the midbrain-hindbrain boundary, interneuron specification, and development of the thyroid gland and kidney (reviewed in Goode and Elgar, 2009). They are also important for development of the otic and epibranchial placodes (reviewed in Baker and Bronner-Fraser, 2001; Schlosser, 2006; Schlosser, 2010). Epibranchial placodes give rise to the visceral sensory neurons of the geniculate, petrosal, and nodose ganglia, i.e., the distal sensory ganglia of cranial nerves VII, IX, and X, respectively (reviewed in Baker and Bronner-Fraser, 2001; Schlosser, 2006; Schlosser, 2010). We examined the expression of paddlefish *Pax2* (Fig. 3), *Pax5* and *Pax8* (Fig. 4) at a variety of developmental stages.

We confirmed that *Pax2* expression in the otic and epibranchial placodes is a highly conserved feature with other gnathostomes (Fig. 3). At stage 24, *Pax2* was clearly but faintly expressed in the otic placodes and strongly expressed at the midbrain-hindbrain boundary, as well as in the developing pronephros (Fig. 3a,b). At stage 26, *Pax2* was strongly expressed

in the medial otic vesicle; it was also maintained in the midbrain-hindbrain boundary and, weakly, in the pronephros (Fig. 3c,d). Furthermore, *Pax2* was now observed in two faint patches in association with the pharyngeal arches (which are themselves located laterally over the yolk at this stage; see Bemis and Grande, 1992): the geniculate placode, developing dorsocaudal to the external position of the first pharyngeal pouch (future position of the first pharyngeal cleft) between the mandibular and hyoid arches, and the petrosal placode, developing dorsocaudal to the future second pharyngeal cleft (Fig. 3d). *Pax2* expression was also observed in the developing optic stalk, and in interneurons within the hindbrain and spinal cord (Fig. 3c,d).

By stage 29, the expression of *Pax2* in the epibranchial placodes was stronger and broader, and included the nodose placodes, developing dorsocaudal to the post-hyoid pharyngeal clefts (Fig. 3e). Expression was maintained in the optic stalk, midbrain-hindbrain boundary, medial otic vesicles and interneurons, but lost in the nephric system. This pattern of expression continued through the “head lifting” process, and by stage 32, *Pax2* expression in the epibranchial placodes could be seen more clearly in lateral view (Fig. 3f). At this stage, transverse sections at the level of the caudal otic vesicle illustrated *Pax2* expression in the medial portion of the otic vesicle, hindbrain interneurons and also the petrosal placode (Fig. 3g-h’). Just as in amphibians (e.g. Schlosser and Ahrens, 2004), neurogenic placodes in paddlefish form in the deep layer of the stratified epithelial ectoderm, adjacent to the basement membrane (Fig. 3g-h’) (also see Bemis and Grande, 1992).

By stage 37, *Pax2* expression in the geniculate, petrosal and first nodose placodes has become restricted dorsally (Fig. 3i; compare with Fig. 3f), relative to broader expression in the second and third (possibly the fused third and fourth) nodose placodes. It is likely that epibranchial placode-derived cells that have already delaminated and differentiated as neurons have downregulated *Pax2*, as seen in chick and zebrafish (Baker and Bronner-Fraser, 2000; Nechiporuk *et al.*, 2007). The other *Pax2* expression domains remained as previously described. By the latest stage examined, stage 46 (the end of the yolk-sac larval stage and beginning of feeding), *Pax2* expression was restricted to the caudalmost nodose placodes (Fig. 3j,k).

Overall, the expression of paddlefish *Pax2* is highly conserved with that of other vertebrates, both in the development of the otic and epibranchial placodes, and in other expression domains such as the optic stalks, midbrain-hindbrain boundary, interneurons and pronephros.

Expression of *Pax8*, but not *Pax5*, is seen during paddlefish otic placode development

In both zebrafish and *Xenopus*, though not in mouse, expression of all the Pax2/5/8 family members is seen in the developing otic placode. Zebrafish *Pax5* is expressed in the anterior otic placode and maintained in the anterior sensory patch, the utricular macula, where it is required for mechanosensory hair cell survival (Kwak *et al.*, 2006; Pfeffer *et al.*, 1998), while transient *Pax5* expression has been reported in the *Xenopus* otic vesicle (Heller and Brändli, 1999). In contrast, *Pax5* expression is not seen in the developing mouse otic placode or vesicle (Bouchard *et al.*, 2010; Pfeffer *et al.*, 1998). Similarly, in paddlefish, *Pax5* expression was not detected in the otic placode, or any other neurogenic placodes, at any

stage of development (Fig. 4a-c). From stage 29 through stage 40, *Pax5* transcripts were restricted to the midbrain-hindbrain boundary, with the strongest expression between stage 29 (Fig. 4a,b) and stage 35. By stage 37, *Pax5* was still observed at the midbrain-hindbrain boundary, and weakly in the hindbrain and spinal cord (Fig. 4c).

Paddlefish *Pax8* was expressed in a pattern very similar to that of *Pax2*, except that no expression was detected in the epibranchial placodes. At stage 24, *Pax8* transcripts were already observed in the otic placode, the midbrain-hindbrain boundary, and the developing pronephros (Fig. 4d,e; compare with *Pax2* expression in Fig. 3a,b). At stage 26, the otic, midbrain-hindbrain boundary, and pronephric expression domains persisted, though as had been seen for *Pax2, Pax8* expression became restricted to the most medial region of the developing otic vesicle (Fig. 4f). *Pax8* expression in the pronephros seemed to be restricted to the pronephric canals adjacent to the somites. The pronephric expression of *Pax8* persisted longer and became stronger as development proceeded, in contrast to that of *Pax2* (Fig. 3c). This was most evident at stage 32, when *Pax8* was strongly expressed in the broadening pronephric canals and ducts (Fig. 4g,h,j,j'). Also at stage 32, *Pax8* expression was seen in interneurons within the hindbrain and spinal cord (Fig. 4g-i). By stage 39, the hindbrain expression of *Pax8* was even more pronounced, with only faint expression persisting in the midbrain-hindbrain boundary and otic vesicle (Fig. 4k). At this stage, a ventromedial spot of *Pax8* expression, which first appeared at stage 35 (not shown), almost certainly represents the developing thyroid gland (Fig. 4k), which develops in this position and expresses *Pax8* and/or *Pax2* in other vertebrates (reviewed in Goode and Elgar, 2009).

Overall, paddlefish *Pax8* expression seems to be well conserved with *Pax8* expression in other vertebrates, both in the otic placode and in other domains such as the midbrain-hindbrain boundary and pronephros. In contrast, expression of paddlefish *Pax5* is not seen in the otic vesicle, as in mouse but unlike zebrafish and *Xenopus*.

Phox2b expression is conserved in epibranchial placode-derived neurons

The homeodomain transcription factor *Phox2b* is a highly conserved marker of epibranchial placode-derived neurons (reviewed in Brunet and Pattyn, 2002). In order to better understand the timing of epibranchial placode formation and neurogenesis in paddlefish, we examined the expression of *Phox2b* (Fig. 5). *Phox2b* transcripts could first be distinguished at stage 26 in a stripe of cells ventrolateral to the rostral hindbrain; these cells represent the first neurons of the developing geniculate ganglion (Fig. 5a,b). *Phox2b*-positive cells were also found in the hindbrain at this stage, presumably in developing motor neurons and interneurons. By stage 29, the *Phox2b*-positive cells in the geniculate ganglion had condensed into a discrete patch of cells and a second, more caudal, domain of expression was seen: the developing petrosal ganglion (Fig. 5c,d). By stage 35, *Phox2b* expression was observed in all the epibranchial placode-derived ganglia, including the developing nodose ganglia, although individual nodose ganglia could not be distinguished at this stage (Fig. 5e-h). *Phox2b* expression in epibranchial placode-derived neurons persisted at stage 39 and ganglion formation was more pronounced (Fig. 5i-l). Individual nodose ganglia could also be distinguished at this stage, both in whole-mount (Fig. 5i,j) and in transverse sections (Fig.

5l). This pattern of expression persisted through stage 46, the latest stage examined (not shown).

Sox3 is a novel marker of electrosensory lateral line organs

Sox3 is a member of the SoxB1 family of HMG domain transcription factors (reviewed in Miyagi *et al.*, 2009). It is expressed in the "posterior placodal area" (Schlosser and Ahrens, 2004) within which the otic, epibranchial and lateral line placodes form (reviewed in Ladher *et al.*, 2010; Schlosser, 2006; Schlosser, 2010). We were particularly interested in examining its expression in paddlefish because of its strong expression in developing lateral line placodes and lateral line primordia in *Xenopus* (Schlosser and Ahrens, 2004), and its reported putative expression in lateral line placodes in medaka and zebrafish (Köster *et al.*, 2000; Nikaido *et al.*, 2007). As previously mentioned, these species only possess the mechanosensory division of the lateral line, while paddlefish also retain the electrosensory division.

Paddlefish *Sox3* expression in the neural plate was evident at the earliest stage examined, stage 24 (Fig. 6a). By stage 26, the neural tube expression domain of *Sox3* was stronger, and two broad lateral domains of *Sox3* expression were visible in the developing pharyngeal arches, over the yolk (Fig. 6b,c): we suggest that these domains represent both the developing epibranchial and lateral line placodes (compare with *Pax2* expression in Fig. 3d). Following the head lift process, *Sox3* expression persisted in the lateral regions, as well as in the central nervous system, and expression was also now seen in the developing olfactory pit (Fig. 6d). By stage 35, *Sox3* expression could be distinguished in both epibranchial placodes and lateral line placodes, in particular the three pre-otic lateral line placodes, i.e., the anterodorsal, anteroventral and otic lateral line placodes, which have already begun to elongate to form sensory ridges (Fig. 6e). A transverse section at the level of the hindbrain, for example, revealed *Sox3*-positive cells in the otic lateral line placode and, more faintly, in the petrosal placode (Fig. 6e,f). From this stage onwards, the boundaries of individual lateral line placodes were difficult to determine owing to the large size of some of the ridges.

In paddlefish, the lateral line system comprises lines of mechanosensory neuromasts on both head and trunk, and fields of electrosensory ampullary organs (which are innervated, like the neuromasts, by lateral line placode-derived neurons) on either side of the cranial lines of neuromasts. By stage 39, *Sox3* expression could be observed in both lines of mechanosensory neuromasts and developing fields of electrosensory ampullary organs (Fig. 6h-j). A transverse section at the level of the eye, for example (Fig. 6i), showed *Sox3* expression in neuromasts of the supraorbital and infraorbital lines, as well as in a broad patch ventral to the infraorbital line, which represents a developing field of ampullary organs (Fig. 6i,j). *Sox3* expression at this stage also highlighted the posterior lateral line placode of the main trunk line, which had begun migrating over the trunk (Fig. 6h,l). Epibranchial placode expression of *Sox3* was weaker and restricted to more dorsal regions of the ectoderm (Fig. 6h). In transverse section, *Sox3* expression was also seen more weakly in cells apparently streaming from the placodes (Fig. 6k), raising the possibility that *Sox3* is maintained in epibranchial placode-derived neurons in paddlefish, in contrast to chick (where it has been proposed that downregulation of *Sox3* is required for cells to leave the

placode and differentiate as neurons; Abu-Elmagd *et al.*, 2001). However, since *Sox3* expression has also been reported in the pharyngeal pouches in *Xenopus* (Schlosser and Ahrens, 2004), this might instead represent conservation of *Sox3* expression in distal pharyngeal pouch endoderm in paddlefish.

From stage 41 onwards, *Sox3* expression in the epibranchial placodes was downregulated and then entirely lost (Fig. 6m,n). However, expression of *Sox3* in the developing lateral line system was maintained and further expanded. By stage 43, the posterior lateral line placode (which only deposits neuromasts) had migrated halfway down the length of the trunk, while in the head, individual *Sox3*-positive ampullary organs were visible (Fig. 6n). At this stage, the lines of neuromasts in the head were already recessed within lateral line canals and *Sox3* expression was no longer visible in these lines. By stage 46, distinct fields of electrosensory ampullary organs could be identified by *Sox3* expression (Fig. 6o-q), and the *Sox3*-positive posterior lateral line primordium was still migrating towards the tail (Fig. 6r).

We did not detect *Sox3* expression within the otic vesicle at any stage in paddlefish: this contrasts with its expression in the neurogenic domain of the otic vesicle in e.g. chick (Neves *et al.*, 2007).

Overall, *Sox3* is a conserved marker for both epibranchial and lateral line placodes in paddlefish. Importantly, it is also a novel vertebrate marker for all stages of development of electrosensory lateral line ampullary organs, and the first published marker for actinopterygian ampullary organs. We will present a comprehensive analysis of paddlefish lateral line development in a subsequent manuscript.

NeuroD is a conserved marker of cranial sensory ganglion development in paddlefish

NeuroD is a basic-helix-loop-helix (bHLH) neurogenic transcription factor that is expressed in neurogenic placode-derived neuroblasts in *Xenopus* and other vertebrates (reviewed inChae *et al.*, 2004), including shark (O'Neill *et al.*, 2007). To better understand the developmental timing of neurogenesis within the neurogenic placodes during paddlefish development, we analyzed the expression of this presumptive pan-neuronal marker (Fig. 7). At stage 26, *NeuroD* expression was observed in multiple domains, suggesting neurogenesis had already begun at an earlier stage (Fig. 7a-c). *NeuroD* expression was seen in two discrete patches of neuroblasts lateral to the midbrain, i.e., the developing profundal and trigeminal ganglia (Fig. 7a,b). The profundal ganglion (located dorsal to the developing trigeminal ganglion) was already more condensed than the more diffuse and larger patch of trigeminal neuroblasts (Fig. 7c), suggesting that profundal neuroblasts differentiate before trigeminal neuroblasts. *NeuroD* expression was also observed at this stage in the olfactory placode, in the eye (presumably in differentiating retinal ganglion cells), in a large domain extending both rostral and medial to the developing otic vesicle and in a smaller faint domain lateral to the otic vesicle (Fig. 7c). Based on its position, and comparison with *Pax2* and *Phox2b* expression (see Fig.3; Fig. 5), we suggest that the large domain of *NeuroD* expression includes neuroblasts of the developing geniculate and vestibuloacoustic ganglia (and potentially also a few lateral line ganglion neuroblasts), while the small domain lateral to the otic vesicle is the developing petrosal ganglion (Fig. 7c).

At stage 29, *NeuroD* expression was maintained in all the above-mentioned domains, and also seen in the epiphysis (future pineal gland) (Fig. 7d,e). The profundal and trigeminal expression domains were more condensed and also weaker, suggesting that neurogenesis in these ganglia was nearly complete by this stage. *NeuroD* expression in the petrosal ganglion region was much stronger and larger, suggesting petrosal placode neurogenesis was at its peak (Fig. 7e). In transverse sections, *NeuroD* expression in the geniculate ganglion and vestibuloacoustic neuroblasts exiting the otic vesicle could be seen clearly (Fig. 7f,g), while petrosal placode-derived neuroblasts were still close to the epithelium, suggesting they had only just begun delaminating (Fig. 7g).

By stage 35, *NeuroD* was weakly expressed in the profundal ganglia, olfactory pit and eye (Fig. 7h), and more strongly expressed in the same large domain extending rostral and medial to the otic vesicle, representing the geniculate, vestibuloacoustic, and presumably also some lateral line ganglia. A new domain of *NeuroD* expression caudal to the eye likely represents neuroblasts of the developing anterodorsal lateral line ganglion.

By stage 39, *NeuroD* expression had been lost in most cranial sensory ganglia, but was still weakly seen in the petrosal ganglion and the first nodose ganglion, and much more strongly in the remaining nodose ganglia (Fig. 7i,j), demonstrating the rostral to caudal wave of neurogenesis within the epibranchial placode-derived ganglia. By stage 46, *NeuroD* transcripts were completely absent, suggesting cranial sensory ganglion neurogenesis was complete by this stage (not shown).

Overall, *NeuroD* expression in paddlefish reveals the dynamic pattern of neurogenesis during cranial sensory ganglion formation and provides a framework for further analysis of this process. A more thorough analysis of neurogenesis would be aided by specific molecular markers distinguishing vestibuloacoustic, lateral line and epibranchial placode-derived ganglia.

DISCUSSION

We have presented the first molecular analysis of neurogenic placode development in a basal actinopterygian fish, *Polyodon spathula* (North American paddlefish). We have confirmed the evolutionary conservation of expression of seven transcription factor genes during neurogenic placode development, including *Pax3* specifically in the profundal placode and ganglion, *Pax2/5/8* family members in the otic and/or epibranchial placodes, *Phox2b* in epibranchial placode-derived neurons, and *Sox3* during epibranchial and lateral line (but not otic) placode development. We have further identified *Sox3* as a novel molecular marker for vertebrate electrosensory ampullary organs, and as the first published marker for actinopterygian ampullary organs.

Pax3 expression in the paddlefish profundal placode confirms its homology with the amniote ophthalmic trigeminal placode

We have shown that *Pax3* is expressed in the profundal placode and ganglion of a basal actinopterygian fish (*Polyodon*). Hence, the profundal placode and ganglion have now been shown to express *Pax3* in chondrichthyans (the shark *Scyliorhinus*; O'Neill *et al.*, 2007) and

in both extant groups of osteichthyans (the actinopterygian *Polyodon*, this article; and the tetrapod sarcopterygian *Xenopus*; Schlosser and Ahrens, 2004), strongly suggesting that the profundal placode and ganglion in the ancestral gnathostome (jawed vertebrate) must also have expressed *Pax3*. In our view, the expression of *Pax3* in the paddlefish profundal placode and ganglion is the final piece of evidence needed to confirm the previously proposed (and much debated) homology of the anamniote profundal placode and ganglion with, respectively, the ophthalmic trigeminal (opV) placode and the ophthalmic lobe of the trigeminal ganglion in amniotes (see discussion in O'Neill *et al.*, 2007; Schlosser, 2006; Schlosser and Northcutt, 2000; Xu *et al.*, 2008). In those vertebrates in which profundal and trigeminal ganglia are fused, therefore, we suggest that *Pax3* expression can be used as a criterion for identifying the profundal placode and profundal placode-derived neurons. An example is the recently reported use of *Pax3* expression to identify putative "ophthalmic trigeminal" placode-derived neurons in the zebrafish trigeminal ganglion (Minchin and Hughes, 2008).

Expression of *Pax2/5/8* family members during paddlefish neurogenic placode development

The Pax2/5/8 family of transcription factors is important for the development of a subset of neurogenic placodes (reviewed in Baker and Bronner-Fraser, 2001; Schlosser, 2006; Schlosser, 2010). The otic, lateral line and epibranchial placodes all seem to develop from a "posterior placodal area" (Schlosser and Ahrens, 2004), characterized by expression of genes including *Pax2, Pax8* and *Sox3* (reviewed in Ladher *et al.*, 2010; Schlosser, 2006; Schlosser, 2010). Although we were unable to detect a posterior placodal area in paddlefish through expression of either *Pax2* or *Pax8, Pax2* is a conserved marker in paddlefish for both the developing otic and epibranchial placodes, as expected from zebrafish, *Xenopus*, chick, and shark (Baker and Bronner-Fraser, 2000; Nechiporuk *et al.*, 2007; O'Neill *et al.*, 2007; Schlosser and Ahrens, 2004). *Pax8*, one of the earliest markers for the otic placode, is jointly required with *Pax2* for otic placode development in zebrafish (Hans *et al.*, 2004; Mackereth *et al.*, 2005) and mouse (Bouchard *et al.*, 2010). In paddlefish, *Pax8* expression within the neurogenic placodes is confined to the otic placode, with no expression seen at any stage in the epibranchial placodes. Similarly, *Pax8* expression in the epibranchial placodes has not been reported in zebrafish (Nikaido *et al.*, 2007; Sun *et al.*, 2007). In *Xenopus, Pax8* expression is only transiently retained in the developing epibranchial placodes (Schlosser and Ahrens, 2004), while genetic lineage tracing in mouse suggests the epibranchial placodes develop from *Pax8*-positive precursors (Bouchard *et al.*, 2004), consistent with *Pax8* expression in the posterior placodal area.

In zebrafish, *Pax5* is expressed in a restricted anterior domain of the otic placode and subsequently in hair cells of the utricular macula, whose survival depends on Pax5 function (Kwak *et al.*, 2006; Pfeffer *et al.*, 1998). In *Xenopus*, weak, transient *Pax5* expression has also been reported in the developing otic vesicle (Heller and Brändli, 1999). In paddlefish, however, as in mouse (see Bouchard *et al.*, 2010), *Pax5* is not expressed at any stage during otic placode development (or indeed during the development of any other placodes).

Sox3 is expressed throughout the development of both mechanosensory and electrosensory divisions of the lateral line system

Sox3 was reported as a particularly strong marker for lateral line placodes and elongating lateral line primordia in *Xenopus* (Schlosser and Ahrens, 2004), and in two teleosts, medaka and zebrafish (Köster *et al.*, 2000; Nikaido *et al.*, 2007). However, *Xenopus*, medaka and zebrafish all lack the electrosensory division of the lateral line system: electrosensory ampullary organs were lost in anuran amphibians (Bullock, 1982; Bullock *et al.*, 1983) and in the actinopterygian radiation leading to teleosts (although electroreception was independently "re-invented" at least twice within different groups of teleosts; Alves-Gomes, 2001; Bullock *et al.*, 1983).

Ampullary organs and the electrosensory hair cells within them were conclusively shown to be derived from lateral line placodes in a tetrapod, the axolotl *Ambystoma mexicanum* (a urodele amphibian), using fate-mapping and ablation studies (Northcutt *et al.*, 1995). In the shark *Scyliorhinus canicula*, electrosensory hair cells were proposed to be neural crest-derived owing to their expression of *Sox8* and the carbohydrate epitope recognized by the HNK1 antibody (Freitas *et al.*, 2006). However, neither of these proposed markers of the neural crest lineage is neural crest-specific (indeed, HNK1 was reported not to label neural crest cells in embryos of a related shark species, *S. torazame*; Kuratani and Horigome, 2000), and gene expression alone does not indicate lineage.

We found that not only is *Sox3* expressed in lateral line placodes and maintained in elongating or migrating lateral line primordia in both head and trunk, as expected from the teleost and frog data (Köster *et al.*, 2000; Nikaido *et al.*, 2007; Schlosser and Ahrens, 2004); it is also broadly expressed in developing ampullary organ fields and maintained in ampullary organs themselves. Only five molecular markers for vertebrate ampullary organs have previously been reported: in axolotl, *Dlx3* and *Msx2* (Metscher *et al.*, 1997), and in sharks, *Eya4* (O'Neill *et al.*, 2007), *Sox8* and *ephrinB2* (Freitas *et al.*, 2006). Hence, *Sox3* is a novel molecular marker for vertebrate ampullary organs, and also the first published molecular marker for actinopterygian ampullary organs. This result is compatible with, though does not prove, a lateral line placode origin for actinopterygian ampullary organs. If true, this would in turn support a lateral line placode origin for ampullary organs in all bony fish, given that ampullary organs are lateral line placode-derived in sarcopterygians (Northcutt *et al.*, 1995). In order to prove a lateral line placode origin for paddlefish ampullary organs, however, *in vivo* fate mapping or labelling studies must be performed during stages of lateral line placode formation and elongation.

METHODS

Collection and staging of paddlefish embryos

Polyodon spathula embryos were purchased from Osage Catfisheries, Inc. (Osage Beach, MO, USA). Embryos were raised at approximately 22°C in tanks with filtered and recirculating water (pH 7.2α0.7, salinity of 1.0α0.2ppt) to desired stages. Staging was done according to Bemis and Grande (1992). Embryos were fixed in either 4% paraformaldehyde in phosphate-buffered saline (PBS) or in modified Carnoy's fixative (6 volumes 100%

ethanol: 3 volumes 37% formaldehyde: 1 volume of glacial acetic acid) for 4 hours at room temperature or overnight at 4°C. Specimens were washed in PBS and then dehydrated stepwise into 100% methanol or ethanol and stored at −20°C.

cDNA synthesis and cloning

RNA from embryos stages 26 to 46 was extracted using Trizol reagent (Invitrogen) and used to generate single strand cDNA using the Superscript III First Strand Synthesis kit (Invitrogen), as per the manufacturer's instructions. Primers were designed either manually from conserved sequence alignments or using iCODEHOP v1.0 (https://icodehop.cphi.washington.edu/icodehop-context/Welcome). The following primers were used (F, forward; R, reverse): *Pax3F*: TACCAGGAGACNGGHTCCAT; *Pax3R*: ACCTGWGTGARAGGCCGTTGC; *Pax2F*: GACCCNTTCTCNKCNATGCA; *Pax2R*: AAYCKCCARGCYTCRTTGTA; *Pax5F*: CATGGAGGRAAYCAGCTDGGKGGNGTKTTTGT; *Pax5*R: TTCATSTCMTCCARNCCNCCRGCYAGHADGCC; *Pax8F*: TGAATGGVCGVCCKCTDCCRGARGTG; *Pax8R*: GCAGCTNTCCTGRTCACTRTCATC; *Phox2bF*: TATAAAATGGANTAYTCTTACCTSAATTCC; *Phox2bR*: GAGGACARNACGSWAGCGAASGGNCC; Sox3*F*: CCGGGTGAAGCGGCCNATGAAYGC; Sox3*R*: CAGGGGCACGGTGCCRTTNACNSC; *NeuroDF*: CCCAARAGRCGVGGNCCCAARAAGAAGAARATGAC; *NeuroDR*: TGRAAKATGGCRTTNAGCTGGGCRCTCATGAC

PCR fragments were cloned into the pDrive cloning vector (Qiagen). Plasmids were purified and sequenced by the Department of Biochemistry DNA Sequencing Facility, University of Cambridge. Sequence results were analyzed using MacVector and BLAST (http://blast.ncbi.nlm.nih.gov/Blast.cgi) prior to phylogenetic analysis. Genbank accession numbers are as follows: *PsNeuroD* HQ690099; *PsPax2* HQ690100; *Ps*Pax3 HQ690101; *PsPax5* HQ690102; *PsPax8* HQ690103; *PsPhox2b* HQ690104; *Ps*Sox3 HQ690105.

Phylogenetic analysis

Amino acid sequences used in phylogenetic analyses were obtained from the National Center for Biotechnology Information (NCBI). Genbank accession numbers for analyses: ***NeuroD***:*Danio rerio* AAB88820; *Gallus gallus* AAC79425; *Homo sapiens* AAA93480; *Mus musculus* NP_035024; *Salmo salar* ACN10533; *Scyliorhinus canicula* ABM89501; *Xenopus laevis* NP_001079263. ***NeuroD2***: *Danio rerio* NP_571157; *Homo sapiens* NP_006151; *Mus musculus* AAH58965. ***Pax3***: *Danio rerio* AAC41253; *Gallus gallus* BAB85652; *Homo sapiens* NP_852122; *Mus musculus* AAH48699*; Scyliorhinus canicula* ABM89502; *Xenopus laevis* AAI08574. ***Pax7***: *Danio rerio* NP_571400; *Gallus gallus* NP_990396; *Homo sapiens* CAA65522; *Mus musculus* AF254422; *Xenopus laevis* NP_001088995. ***Pax2***: *Danio rerio 2a* NP571259; *Danio rerio 2b* NP571715; *Gallus gallus* NP_990124; *Homo sapiens* AAC63385**;** *Mus musculus* CAA39302**;** *Oryzias latipes* CAB09696**;** *Scyliorhinus canicula* ABM89503**;** *Xenopus laevis 2a* NP_001079830; *Xenopus laevis 2b* O57682. ***Pax5***: *Danio rerio* NP571713.1; *Gallus gallus* BAA76951; *Homo sapiens*

NP_057953; *Mus musculus* NP_032808; *Xenopus laevis* NP_001079237. ***Pax8***: Danio *rerio* XP_001339893; *Homo sapiens* AAB34216*; Mus musculus* CAA40725*; Takifugu rubripes* AAC31810*; Xenopus laevis* NP_001081941. ***Phox2a***: *Danio rerio* NP_996953; *Homo sapiens* NP_005160; *Mus musculus* Q62066; *Xenopus laevis* AAI24892. ***Phox2b***: *Danio rerio* NP_001014818; *Homo sapiens* NP_003915; *Mus musculus* CAA74833; *Scyliorhinus canicula* ABM89504; *Xenopus laevis* NP_001084383. ***Sox1***: *Gallus gallus* BAA25092; *Homo sapiens* NP_005977; *Mus musculus* BAC75667; *Xenopus laevis* BAE72677. ***Sox2***: *Danio rerio* BAE48583; *Gallus gallus* BAC67545; *Homo sapiens* NP_003097; *Mus musculus* AAC31791; *Takifugu rubripes* AAQ18495; *Xenopus laevis* NP_001081691. ***Sox3***: *Danio rerio* BAD11369; *Gallus gallus* BAA25093; *Homo sapiens* CAA50465; *Mus musculus* AAL40744; *Takifugu rubripes* AAQ18496; *Xenopus laevis* AAH72222. We aligned the amino acid sequences for each gene with MUSCLE (Edgar, 2004) and checked them in MacClade v.4.08 (Maddison and Maddison, 2000). We determined the best-fit evolutionary model for each data set in ProtTest v2.4 (Abascal *et al.*, 2005). Phylogenetic analyses were performed under a Bayesian-coalescence framework, implemented in the software BEAST v1.6.1 (Drummond and Rambaut, 2007). One of the advantages of this method is that outgroups are not necessary to root the phylogenetic tree: this is important since it is not trivial to select appropriate outgroups while determining the orthologous or paralogous nature of genes or gene families. BEAST v1.6.1 recovers the genealogy of alleles using the coalescent as a demographic model and a relaxed molecular clock to estimate the substitution rates among branches and, thus, the root of the tree. The search is performed under a Bayesian approach, which results in a set of posterior distributions and credibility intervals for each parameter, including the root and the nodes of each tree.

Analyses in BEAST v1.6.1 were performed using a Yule model of speciation as a prior for the tree, an uncorrelated lognormal clock as a prior for the molecular clock (which permits the relative substitution rates to vary among branches), and the values obtained for the best-fit models in ProtTest as priors for the parameters of the models. We ran the analyses for 2×10^6 generations, sampling every 100 generations to approximate the posterior distribution of the parameters. We analyzed the proper convergence of the MCMC chains in Tracer v1.5 (BEAST v1.6.1 software package). We also removed the first 200 generations as burn-in, after visualizing the log-likelihoods associated with the posterior probabilities again in Tracer v1.5. The remaining trees were summarized in TreeAnnotator v1.6.1 (BEAST v1.6.1 software package), yielding a maximum clade credibility tree with the posterior probabilities annotated for each clade. We contrasted the results with other phylogenetic methods [Maximum Likelihood, as implemented in PhyML 3.0 (Guindon and Gascuel, 2003)]. Results were highly concordant respecting the phylogenetic position of the *Polyodon* genes analyzed (results not shown).

Whole-mount *in situ* hybridization

Antisense RNA probes were generated using T7 or SP6 polymerases (Roche) and digoxigenin- or fluorescein-conjugated dUTPs (Roche). Embryos were rehydrated stepwise into phosphate-buffered saline (PBS) with 0.1% Tween-20 (PTw), bleached in bleaching solution (0.5% SSC, 10% H_2O_2, 5% formamide) under strong white light for 30-60 minutes, depending on stage, and rinsed several times in PTw. After proteinase K treatment

(14-22μg/ml of Roche proteinase K) for 10-15 minutes at room temperature, and two rinses in PTw, embryos were re-fixed in 4% paraformaldehyde with 0.02% glutaraldehyde for 1 hour, rinsed four times with PTw, and then graded into hybridization solution (1x salt solution [0.2 M NaCl, 10 mM Tris, pH 7.5, 5 mM $NaH_2PO_4H_2O$, 5 mM Na_2HPO_4, 5 mM EDTA], 50% formamide, 10% dextran sulphate, 1 mg/ml yeast tRNA, 1x Denhardt's solution). Embryos were pre-hybridized for at least 3 hours at 70°C before the addition of diluted probe in hybridization solution. Embryos were incubated at 70°C in probe solution for at least 18 hours. Post-hybridization procedure was as described in Nikitina *et al.* (2009).

Sectioning embryos after whole-mount *in situ* hybridization

Embryos were incubated in 5% sucrose in PBS for 5 hours at room temperature, then in 15% sucrose in PBS overnight at 4°C, followed by transfer into prewarmed 7.5% gelatin in 15% sucrose in PBS solution and overnight incubation at 37°C. After embedding in molds for transverse sectioning, molds were immersed in a dry ice and isopentane solution for one minute to freeze the gelatin, and the embryos were cryosectioned at 20μm intervals. After 24 hours at room temperature, the gelatin was removed by incubating the slides for 5 minutes in PBS prewarmed to 37°C. The sections were then counterstained with the nuclear marker DAPI (1 ng/ml) and mounted in Fluoromount G (Southern Biotech.).

Acknowledgments

We thank Dr Marcus C. Davis (Kennesaw State University, Georgia) for his assistance in paddlefish embryology and husbandry and Steve Kahrs at Osage Catfisheries Inc. for embryos. We thank Dr Perrine Barraud and Dr Andrew Gillis for helpful discussions and comments on the manuscript. This work was supported by BBSRC grant BB/F00818X/1 to C.V.H.B.

REFERENCES

Abascal F, Zardoya R, Posada D. ProtTest: selection of best-fit models of protein evolution. Bioinformatics. 2005; 21:2104–2105. [PubMed: 15647292]

Abu-Elmagd M, Ishii Y, Cheung M, Rex M, Le Rouëdec D, Scotting PJ. cSox3 expression and neurogenesis in the epibranchial placodes. Dev Biol. 2001; 237:258–269. [PubMed: 11543612]

Alves-Gomes JA. The evolution of electroreception and bioelectrogenesis in teleost fish: a phylogenetic perspective. J Fish Biol. 2001; 58:1489–1511.

Baker CVH, Bronner-Fraser M. Establishing neuronal identity in vertebrate neurogenic placodes. Development. 2000; 127:3045–3056. [PubMed: 10862742]

Baker CVH, Bronner-Fraser M. Vertebrate cranial placodes I. Embryonic induction. Dev Biol. 2001; 232:1–61. [PubMed: 11254347]

Baker CVH, O'Neill P, McCole RB. Lateral line, otic and epibranchial placodes: developmental and evolutionary links? J Exp Zool B Mol Dev Evol. 2008; 310B:370–383. [PubMed: 17638322]

Ballard WW, Needham RG. Normal embryonic stages of *Polyodon spathula* (Walbaum). J Morph. 1964; 114:465–477. [PubMed: 14165136]

Bemis WE, Grande L. Early development of the actinopterygian head. I. External development and staging of the paddlefish *Polyodon spathula*. J Morphol. 1992; 213:47–83.

Bouchard M, de Caprona D, Busslinger M, Xu P, Fritzsch B. Pax2 and Pax8 cooperate in mouse inner ear morphogenesis and innervation. BMC Dev Biol. 2010; 10:89. [PubMed: 20727173]

Bouchard M, Souabni A, Busslinger M. Tissue-specific expression of cre recombinase from the *Pax8* locus. Genesis. 2004; 38:105–109. [PubMed: 15048807]

Brunet J-F, Pattyn A. *Phox2* genes - from patterning to connectivity. Curr Opin Genet Dev. 2002; 12:435–440. [PubMed: 12100889]

Bullock TH. Electroreception. Annu Rev Neurosci. 1982; 5:121–170. [PubMed: 6280574]

Bullock TH, Bodznick DA, Northcutt RG. The phylogenetic distribution of electroreception: evidence for convergent evolution of a primitive vertebrate sense modality. Brain Res. 1983; 287:25–46. [PubMed: 6616267]

Chae JH, Stein GH, Lee JE. NeuroD: the predicted and the surprising. Mol Cells. 2004; 18:271–288. [PubMed: 15650322]

Davis MC, Dahn RD, Shubin NH. An autopodial-like pattern of *Hox* expression in the fins of a basal actinopterygian fish. Nature. 2007; 447:473–476. [PubMed: 17522683]

Davis MC, Shubin NH, Force A. Pectoral fin and girdle development in the basal actinopterygians *Polyodon spathula* and *Acipenser transmontanus*. J Morphol. 2004; 262:608–628. [PubMed: 15376275]

Drummond AJ, Rambaut A. BEAST: Bayesian evolutionary analysis by sampling trees. BMC Evol Biol. 2007; 7:214. [PubMed: 17996036]

Edgar RC. MUSCLE: a multiple sequence alignment method with reduced time and space complexity. BMC Bioinformatics. 2004; 5:113. [PubMed: 15318951]

Freitas R, Zhang G, Albert JS, Evans DH, Cohn MJ. Developmental origin of shark electrosensory organs. Evol Dev. 2006; 8:74–80. [PubMed: 16409384]

Ghysen A, Dambly-Chaudière C. The lateral line microcosmos. Genes Dev. 2007; 21:2118–2130. [PubMed: 17785522]

Goode DK, Elgar G. The *PAX258* gene subfamily: a comparative perspective. Dev Dyn. 2009; 238:2951–2974. [PubMed: 19924770]

Guindon S, Gascuel O. A simple, fast, and accurate algorithm to estimate large phylogenies by maximum likelihood. Syst Biol. 2003; 52:696–704. [PubMed: 14530136]

Hans S, Liu D, Westerfield M. Pax8 and Pax2a function synergistically in otic specification, downstream of the Foxi1 and Dlx3b transcription factors. Development. 2004; 131:5091–5102. [PubMed: 15459102]

Heller N, Brändli AW. *Xenopus Pax-2/5/8* orthologues: novel insights into *Pax* gene evolution and identification of *Pax-8* as the earliest marker for otic and pronephric cell lineages. Dev Genet. 1999; 24:208–219. [PubMed: 10322629]

Hurley IA, Mueller RL, Dunn KA, Schmidt EJ, Friedman M, Ho RK, Prince VE, Yang Z, Thomas MG, Coates MI. A new time-scale for ray-finned fish evolution. Proc R Soc B. 2007; 274:489–498.

Inoue JG, Miya M, Tsukamoto K, Nishida M. Basal actinopterygian relationships: a mitogenomic perspective on the phylogeny of the “ancient fish”. Mol Phylogenet Evol. 2003; 26:110–120. [PubMed: 12470943]

Jørgensen, JM. Morphology of electroreceptive sensory organs. Bullock, TH.; Hopkins, CD.; Popper, AN.; Fay, RR., editors. Electroreception; New York: Springer: 2005. p. 47-67.

Köster RW, Kühnlein RP, Wittbrodt J. Ectopic *Sox3* activity elicits sensory placode formation. Mech Dev. 2000; 95:175–187. [PubMed: 10906460]

Kuratani S, Horigome N. Developmental morphology of branchiomeric nerves in a cat shark, *Scyliorhinus torazame*, with special reference to rhombomeres, cephalic mesoderm, and distribution patterns of cephalic crest cells. Zool Sci. 2000; 17:893–909.

Kwak S-J, Vemaraju S, Moorman SJ, Zeddies D, Popper AN, Riley BB. Zebrafish *pax5* regulates development of the utricular macula and vestibular function. Dev Dyn. 2006; 235:3026–3038. [PubMed: 17013878]

Ladher RK, O’Neill P, Begbie J. From shared lineage to distinct functions: the development of the inner ear and epibranchial placodes. Development. 2010; 137:1777–1785. [PubMed: 20460364]

Ma EY, Raible DW. Signaling pathways regulating zebrafish lateral line development. Curr Biol. 2009; 19:R381–6. [PubMed: 19439264]

Mackereth MD, Kwak SJ, Fritz A, Riley BB. Zebrafish *pax8* is required for otic placode induction and plays a redundant role with Pax2 genes in the maintenance of the otic placode. Development. 2005; 132:371–382. [PubMed: 15604103]

Maddison, DR.; Maddison, WP. MacClade 4: Analysis of phylogeny and character evolution. Sinauer Associates; Sunderland, MA: 2000. Version 4.08

Metscher BD, Northcutt RG, Gardiner DM, Bryant SV. Homeobox genes in axolotl lateral line placodes and neuromasts. Dev Genes Evol. 1997; 207:287–295.

Minchin JE, Hughes SM. Sequential actions of Pax3 and Pax7 drive xanthophore development in zebrafish neural crest. Dev Biol. 2008; 317:508–522. [PubMed: 18417109]

Miyagi S, Kato H, Okuda A. Role of SoxB1 transcription factors in development. Cell Mol Life Sci. 2009; 66:3675–3684. [PubMed: 19633813]

Nechiporuk A, Linbo T, Poss KD, Raible DW. Specification of epibranchial placodes in zebrafish. Development. 2007; 134:611–623. [PubMed: 17215310]

Neves J, Kamaid A, Alsina B, Giráldez F. Differential expression of Sox2 and Sox3 in neuronal and sensory progenitors of the developing inner ear of the chick. J Comp Neurol. 2007; 503:487–500. [PubMed: 17534940]

Nikaido M, Doi K, Shimizu T, Hibi M, Kikuchi Y, Yamasu K. Initial specification of the epibranchial placode in zebrafish embryos depends on the fibroblast growth factor signal. Dev Dyn. 2007; 236:564–571. [PubMed: 17195184]

Nikitina N, Bronner-Fraser M, Sauka-Spengler T. The sea lamprey *Petromyzon marinus*: a model for evolutionary and developmental biology. CSH Protoc. 2009; 2009 pdb.emo113.

Northcutt RG. Evolution of gnathostome lateral line ontogenies. Brain Behav Evol. 1997; 50:25–37. [PubMed: 9209764]

Northcutt RG, Brändle K, Fritzsch B. Electroreceptors and mechanosensory lateral line organs arise from single placodes in axolotls. Dev Biol. 1995; 168:358–373. [PubMed: 7729575]

O'Neill P, McCole RB, Baker CVH. A molecular analysis of neurogenic placode and cranial sensory ganglion development in the shark, *Scyliorhinus canicula*. Dev Biol. 2007; 304:156–181. [PubMed: 17234174]

Pfeffer PL, Gerster T, Lun K, Brand M, Busslinger M. Characterization of three novel members of the zebrafish *Pax2/5/8* family: dependency of *Pax5* and *Pax8* expression on the *Pax2.1* (*noi*) function. Development. 1998; 125:3063–3074. [PubMed: 9671580]

Schlosser G. Making senses development of vertebrate cranial placodes. Int Rev Cell Mol Biol. 2010; 283:129–234. [PubMed: 20801420]

Schlosser G. Development and evolution of lateral line placodes in amphibians I. Development. Zoology (Jena). 2002; 105:119–146.

Schlosser G. Induction and specification of cranial placodes. Dev Biol. 2006; 294:303–351. [PubMed: 16677629]

Schlosser G, Ahrens K. Molecular anatomy of placode development in *Xenopus laevis*. Dev Biol. 2004; 271:439–466. [PubMed: 15223346]

Schlosser G, Northcutt RG. Development of neurogenic placodes in *Xenopus laevis*. J Comp Neurol. 2000; 418:121–146. [PubMed: 10701439]

Streit A. The preplacodal region: an ectodermal domain with multipotential progenitors that contribute to sense organs and cranial sensory ganglia. Int J Dev Biol. 2007; 51:447–461. [PubMed: 17891708]

Sun S-K, Dee CT, Tripathi VB, Rengifo A, Hirst CS, Scotting PJ. Epibranchial and otic placodes are induced by a common Fgf signal, but their subsequent development is independent. Dev Biol. 2007; 303:675–686. [PubMed: 17222818]

Venkatesh B, Erdmann MV, Brenner S. Molecular synapomorphies resolve evolutionary relationships of extant jawed vertebrates. Proc Natl Acad Sci USA. 2001; 98:11382–11387. [PubMed: 11553795]

Wilkens LA, Russell DF, Pei X, Gurgens C. The paddlefish rostrum functions as an electrosensory antenna in plankton feeding. Proc Biol Sci. 1997; 264:1723–1729.

Wojtenek W, Pei X, Wilkens LA. Paddlefish strike at artificial dipoles simulating the weak electric fields of planktonic prey. J Exp Biol. 2001; 204:1391–1399. [PubMed: 11273801]

Xu H, Dude CM, Baker CVH. Fine-grained fate maps for the ophthalmic and maxillomandibular trigeminal placodes in the chick embryo. Dev Biol. 2008; 317:174–186. [PubMed: 18367162]

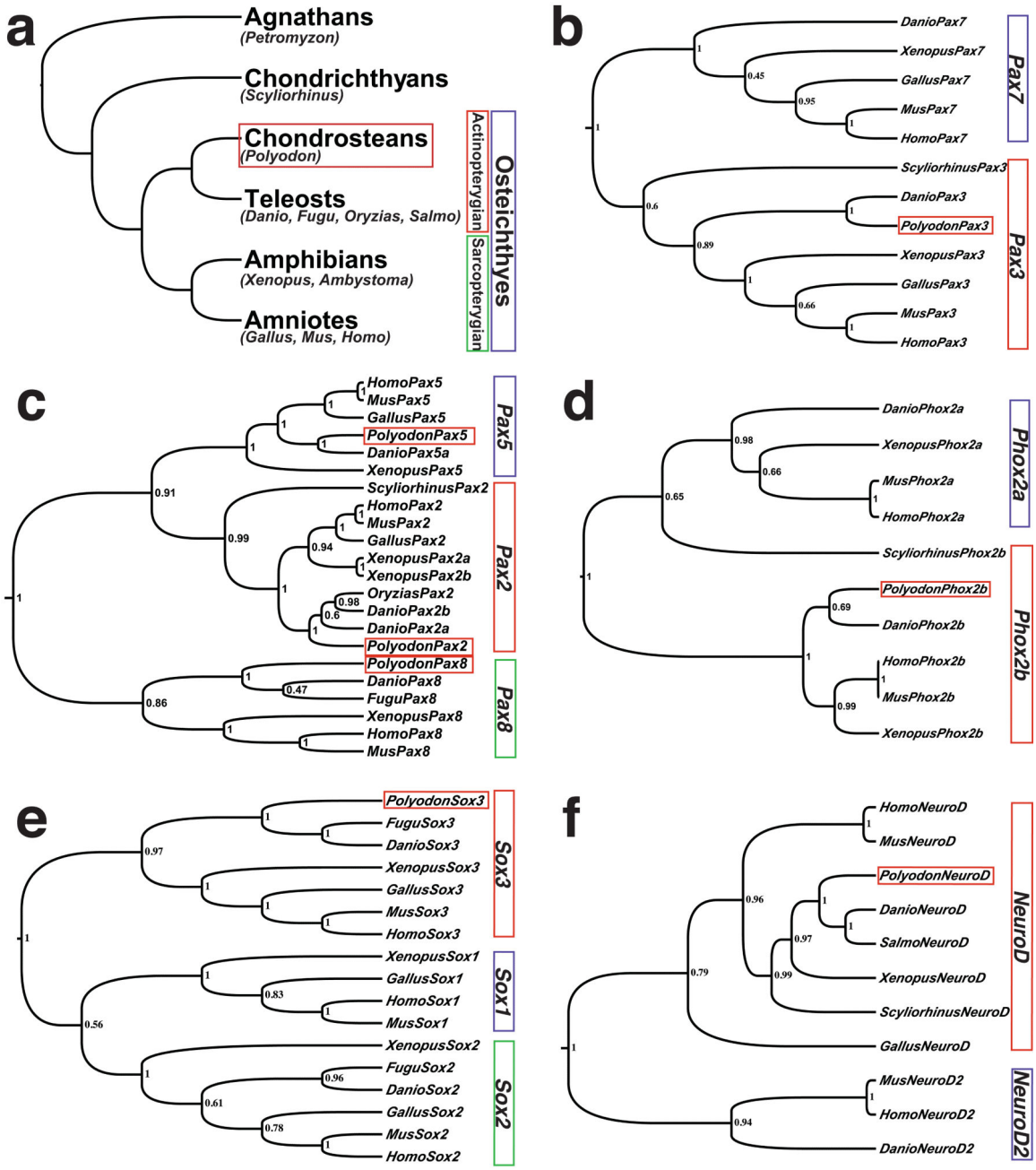

Fig. 1. Phylogenetic trees generated using a Bayesian-coalescence framework confirm the orthology of cloned *Polyodon spathula* (paddlefish) cDNA fragments

(**a**) A highly simplified vertebrate phylogeny showing the relationship of the main vertebrate developmental and genetic model systems in relation to the chondrostean (basal acintopterygian) *Polyodon spathula* (North American paddlefish) (red box), as well as other basal vertebrates used in comparative developmental studies, such as the lamprey *Petromyzon marinus* (an agnathan, *i.e.*, jawless fish), and the shark *Scyliorhinus canicula* (a chondrichthyan, *i.e.*, cartilaginous fish). Tetrapods (amphibians and amniotes) and teleosts are members, respectively, of the two sister groups of bony fish: sarcopterygians (lobe-finned fish) and actinopterygians (ray-finned fish). (**b-f**) Phylogenetic trees showing the

Europe PMC Funders Author Manuscripts

orthology of the *Polyodon* gene fragment with other vertebrates. *Polyodon* sequences are outlined by a red box. Numbers at nodes represent the Bayesian posterior probability of each clade. (**b**) *Pax3*. (**c**) *Pax2/5/8* family. (**d**) *Phox2b*. (**e**) *Sox3*. (**f**) *NeuroD*. Species abbreviations are as follows: *Danio, Danio rerio* (zebrafish)*; Fugu, Takifugu rubripes* (pufferfish)*; Gallus, Gallus gallus* (chicken)*; Homo, Homo sapiens* (human); *Mus, Mus musculus* (mouse)*; Oryzias, Oryzias latipes* (medaka); *Polyodon, Polyodon spathula* (paddlefish); *Salmo, Salmo salmo* (salmon); *Scyliorhinus, Scyliorhinus canicula* (lesser-spotted dogfish/catshark); *Xenopus, Xenopus laevis* (African clawed frog).

Europe PMC Funders Author Manuscripts

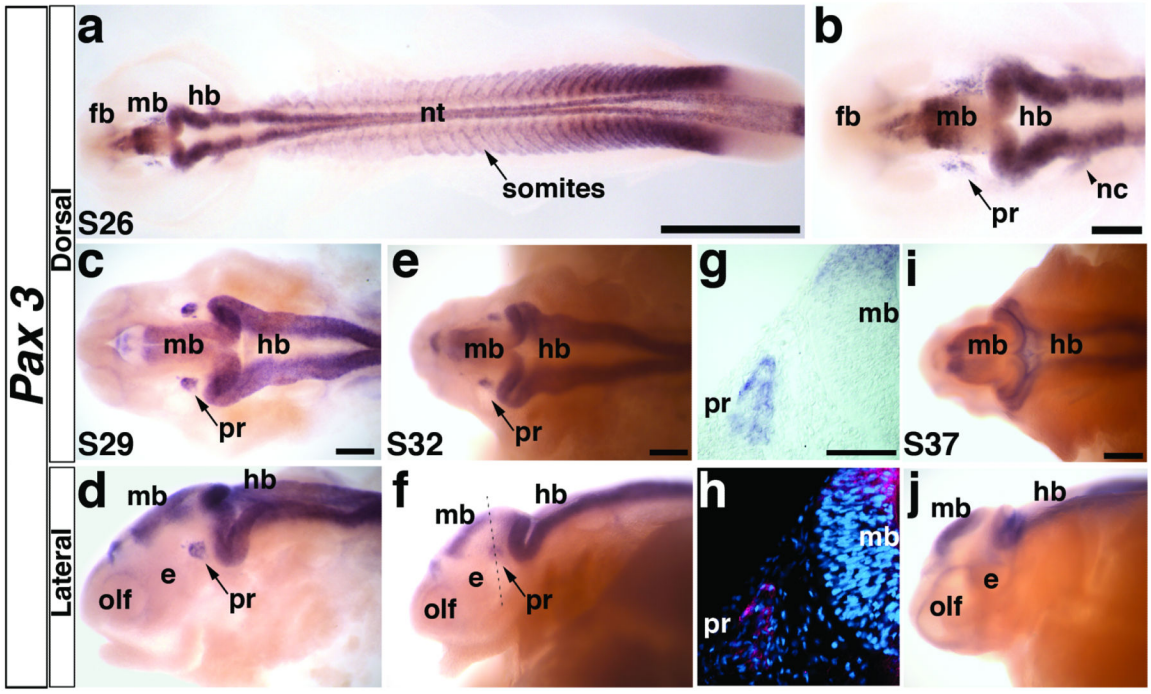

Fig. 2. Paddlefish *Pax3* is expressed in the profundal placode and ganglion

(**a**) Embryo at stage 26 showing the distribution of *Pax3* transcripts in the neural tube, somites, and head. At this stage, the primary divisions of the head into forebrain (fb), midbrain (mb) and hindbrain (hb) are evident. (**b**) Higher power view of head region in panel **a**. *Pax3* is expressed in bilateral patches of cells lateral to the midbrain (mb) in the profundal placode (pr) and in neural crest cells (nc) migrating from the hindbrain (hb) towards the pharyngeal arches. (**c,d**) Stage 29 embryo in dorsal and lateral views, respectively. The *Pax3*-positive cells in the profundal placode (pr) have condensed, yet remain near the epithelium. *Pax3* is also weakly expressed in the olfactory pits (olf). (**e,f**) Stage 32 embryo in dorsal and lateral views. The *Pax3*-positive cells have delaminated from the epithelium into the mesenchyme in the developing profundal ganglion (pr). Dotted line shows plane of section shown in panels **g** and **h**. (**g**) Brightfield image of a transverse section through the stage 32 embryo shown in panel **f**. *Pax3*-positive cells are clearly expressed in the developing profundal ganglion (pr). (**h**) Corresponding false color overlay image of brightfield image in panel **g** (red, *Pax3*) with the nuclear marker DAPI (blue). (**i,j**) Stage 37 embryo in dorsal and lateral views. *Pax3* expression persists in the central nervous system, yet is completely absent in the profundal ganglion by this stage. Abbreviations: **e**, eye; **fb**, forebrain **hb**, hindbrain; **mb**, midbrain; **nt**, neural tube; **olf**, olfactory pits; **pr**, profundal placode or ganglion; **s**, stage. Scale bars: (a) 1 mm; (b-f, i, j) 200 μm; (g,h) 50 μm.

Europe PMC Funders Author Manuscripts

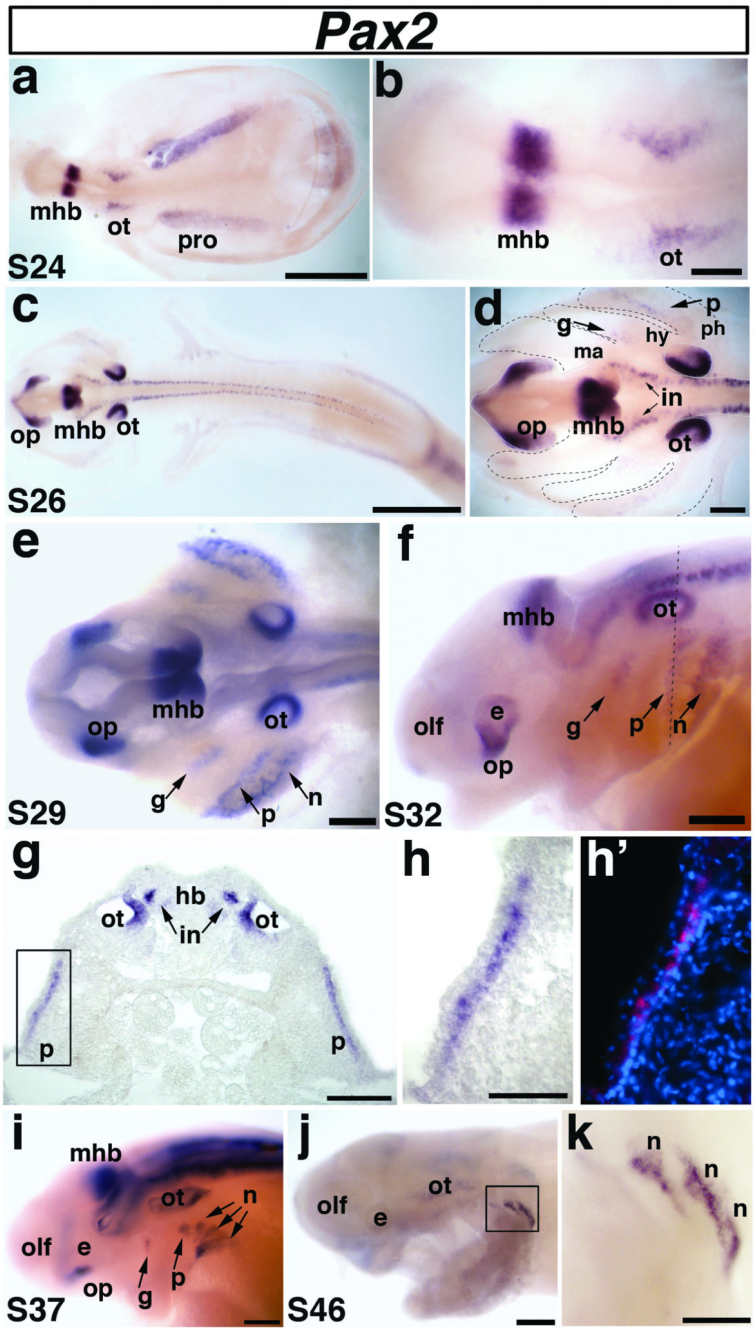

Fig. 3. Paddlefish *Pax2* is expressed in the otic and epibranchial placodes

(**a**) Dorsal view of a stage 24 embryo. *Pax2* is expressed in the midbrain-hindbrain boundary (mhb), the otic placode (ot), and the pronephros (pro). (**b**) Higher power view of the head region in panel **a** shows *Pax2* expression in the otic placode (ot) and midbrain-hindbrain boundary (mhb). (**c**) Dorsal view of a stage 26 embryo. (**d**) Higher power view of head region in panel **c**. *Pax2* continues to be strongly expressed in the midbrain-hindbrain boundary (mhb) and the developing otic vesicle (ot), but has been downregulated in the pronephros (pro). New domains of *Pax2* expression are also present in the optic stalk (op),

and interneurons (in) of the hindbrain and spinal cord, as well as in the developing geniculate (g) and petrosal (p) epibranchial placodes. *Pax2* expression highlights the geniculate placode (g), which is forming dorsocaudal to the external position of the first pharyngeal pouch (i.e., future position of the first pharyngeal cleft) between the mandibular (ma) and hyoid (hy) arches (boundaries indicated with black dashed lines). The developing petrosal placode (p) is located dorsocaudal to the future second pharyngeal cleft between the hyoid (hy) and post-hyoid arches (ph). (**e**) Dorsal view of a stage 29 embryo. *Pax2* continues to be expressed in the previously described domains, with stronger expression within the developing epibranchial placodes, now including the nodose placodes (n) developing caudal to the future third pharyngeal cleft. (**f**). Lateral view of a stage 32 embryo. *Pax2* expression continues in all domains. Dotted line shows plane of section shown in panels **g-h'**. (**g-h'**) Transverse section through the stage 32 embryo shown in panel **f**. (**g**) *Pax2* is expressed in the medial region of the otic vesicle (ot), interneurons (in) of the hindbrain (hb), and in the petrosal placode (p). (**h**) Higher power view of the petrosal placode (p) from panel **g** in brightfield and (**h'**) corresponding false color overlay (red) with DAPI (blue). *Pax2* is only seen in the deep layer of the stratified epithelial ectoderm, adjacent to the basement membrane. (**i**) Lateral view of a stage 37 embryo. The expression of *Pax2* in the nodose placodes has resolved further into three distinct domains representing individual nodose placodes. (**j**) Lateral view of a stage 46 embryo and (**k**) higher power view of boxed area in panel **j**. *Pax2* expression is restricted to the caudalmost nodose placodes. Abbreviations: **e**, eye; **g**, geniculate; **hb**, hindbrain; **hy**, hyoid arch; **in**, interneurons; **ma**, mandibular arch; **mhb**, midbrain-hindbrain boundary; **n**, nodose; **olf**, olfactory pits; **op**, optic stalk; **ot**, otic; **p**, petrosal; **ph**, post-hyoid arches; **pro**, pronephros; **s**, stage. Scale bars: (a,c) 1 mm; (b-f, i,j) 200 μm; (g,k) 100 μm; (h,h') 50 μm.

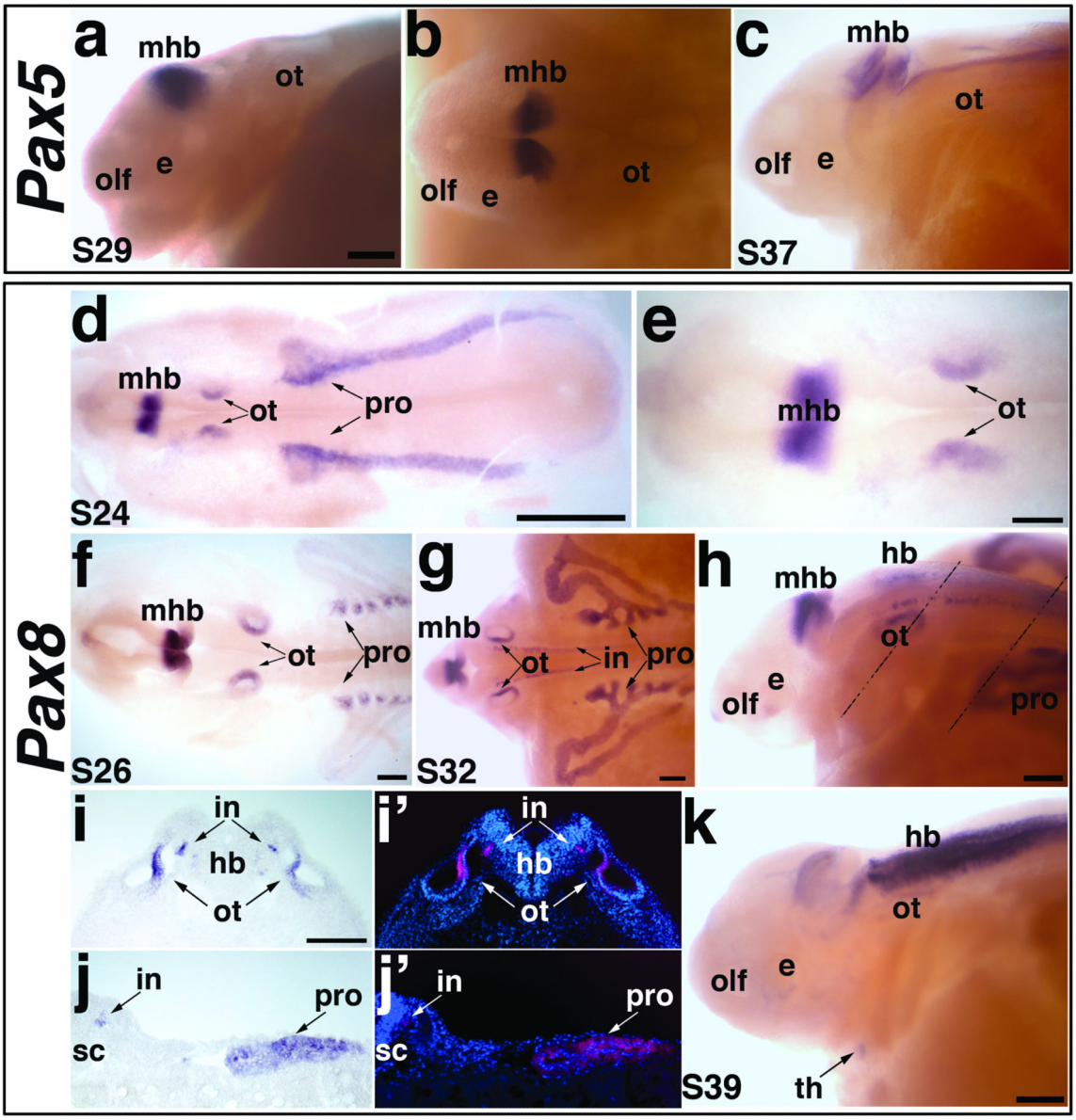

Fig. 4. Paddlefish *Pax5* and *Pax8* expression during otic placode and pronephros development

(**a-c**) *Pax5* expression in paddlefish. (**a,b**) A stage 29 embryo, in lateral and dorsal views, respectively, showing *Pax5* expression. *Pax5* is not expressed in any placodes, but is expressed in the midbrain-hindbrain boundary (mhb). (**c**) Lateral view of a stage 37 embryo. *Pax5* expression is maintained in the midbrain-hindbrain boundary, and more weakly seen in the hindbrain and spinal cord. (**d-k**) *Pax8* expression in paddlefish. (**d**) Dorsal view of a stage 24 embryo showing *Pax8* expression. *Pax8* is restricted to the midbrain-hindbrain boundary (mhb), the otic vesicle (ot), and the developing pronephros (pro). (**e**) Higher power view of head region from panel **d**, showing *Pax8* in the midbrain-hindbrain boundary (mhb) and otic vesicle (ot). (**f**) Dorsal view of a stage 26 embryo. *Pax8* is maintained in the previously described domains. In the elaborating pronephros, *Pax8* appears restricted specifically to the pronephric canals, adjacent to the somites. (**g,h**) Dorsal and lateral views

of a stage 32 embryo. *Pax8* expression is maintained in the midbrain-hindbrain boundary (mhb), otic vesicle (ot) and pronephros (pro). *Pax8* is also strongly expressed in the broadening pronephric canals and ducts and in the interneurons (in) of the hindbrain (hb) and spinal cord (sc). Dotted lines in panel **h** show planes of sections shown in panels **i-i'** and **j-j'**. (**i**) Brightfield image and **(i')** corresponding false color overlay image (red, *Pax8*) with DAPI (blue) showing a section through the otic vesicle of the stage 32 embryo shown in panel **h**. *Pax8* is expressed in a medial region of the otic vesicle (ot) and interneurons (in) of the hindbrain (hb). (**j**) Brightfield image and **(j')** corresponding false color overlay image (red, *Pax8*) with DAPI (blue) showing a section through the pronephros of the stage 32 embryo shown in panel **h**. *Pax8* is observed in the interneurons (in) and pronephric duct (pro). (**k**). Lateral view of a stage 39 embryo. *Pax8* is weakly expressed in the otic vesicle (ot); expression in the hindbrain (hb) has broadened extensively. *Pax8* is also expressed in the putative developing thyroid gland (arrow). Abbreviations: **e**, eye; **hb**, hindbrain; **in**, interneurons; **mhb**, midbrain-hindbrain boundary; **olf**, olfactory pits; **ot**, otic; **pro**, pronephros; **s**, stage; **sc**, spinal cord, **th**, thyroid gland. Scale bars: (a-c) 200 μm; (d) 1 mm; (e-h,k) 200 μm; (i,j) 100 μm.

Europe PMC Funders Author Manuscripts

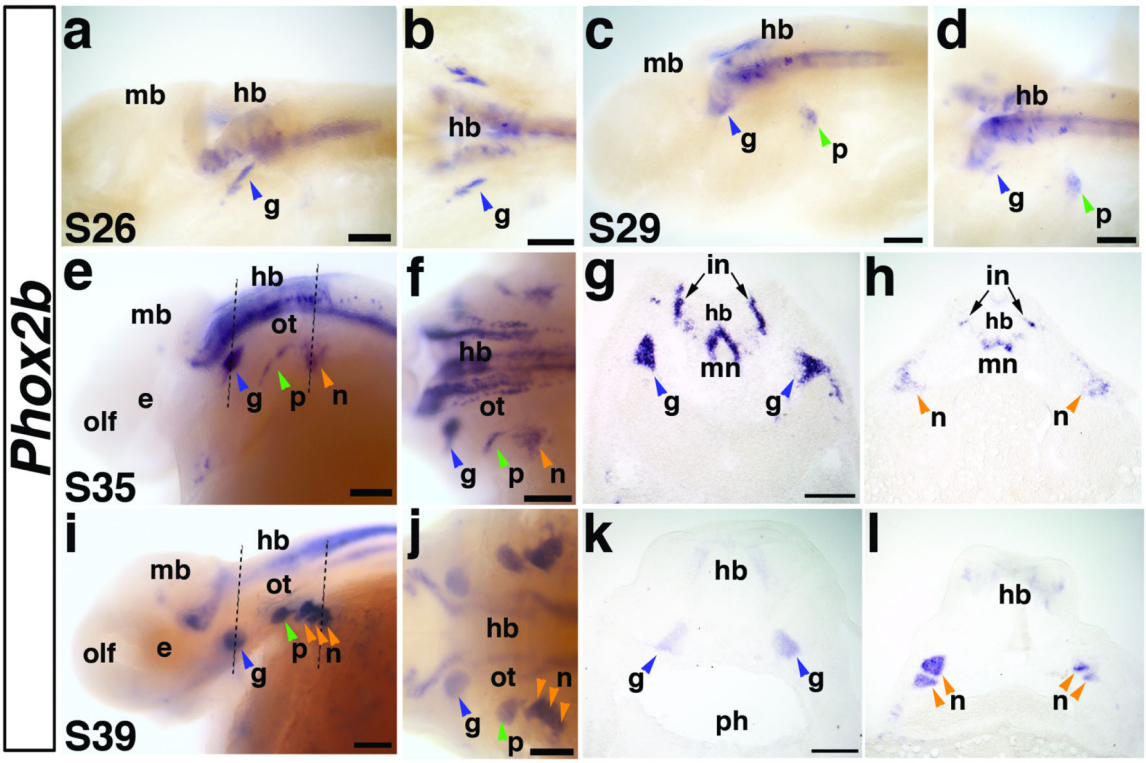

Fig. 5. Paddlefish *Phox2b* is expressed in epibranchial placode-derived neurons

(**a,b**) Lateral and dorsal views, respectively, of a stage 26 embryo. *Phox2b* is expressed in a stripe of cells representing the first neurons of the developing geniculate ganglion (g) (blue arrowhead) and in neurons in the developing hindbrain (hb). Expression of *Phox2b* in the hindbrain (hb) persists throughout embryogenesis. (**c,d**) Lateral and dorsal views of a stage 29 embryo. *Phox2b* is expressed in the condensing geniculate ganglion (blue arrowhead) and now also in the developing petrosal ganglion (p) (green arrowhead). (**e,f**) Lateral and dorsal views of a stage 35 embryo. *Phox2b* expression continues in the geniculate ganglion (blue arrowhead), petrosal ganglion (green arrowhead), and has begun in a patch of cells representing the developing nodose ganglia (n) (orange arrowhead). Dotted lines in panel **e** indicate planes of sections shown in panels **g** and **h**. (**g**) Section through the geniculate ganglia (blue arrowheads) of the stage 35 embryo shown in panels **e,f**. *Phox2b* transcripts are strongly expressed in the geniculate ganglia, as well as in a subset of hindbrain neurons, presumably including interneurons (in) and motor neurons (mn). (**h**) Section through the developing nodose ganglia (orange arrow) in the stage 35 embryo shown in panel **e**. Compared to the condensed geniculate ganglion, *Phox2b*-positive cells of the developing nodose ganglia are still scattered, such that individual ganglia cannot be distinguished. (**i,j**) Lateral and dorsal views of a stage 39 embryo. *Phox2b* expression clearly marks all the condensed epibranchial placode-derived ganglia (arrowheads). Dotted lines in panel **i** indicate planes of sections in panels **k** and **l**. (**k**) Section through the geniculate ganglia (blue arrowheads) of the stage 39 embryo shown in panels **i,j**, showing *Phox2b* expression in the medially located ganglia. (**l**) Section through the nodose ganglia (orange arrowheads) of the stage 39 embryo shown in panels **i,j**. At this stage, individual *Phox2b*-positive nodose ganglia can be distinguished. Abbreviations: **e**, eye; **g**, geniculate ganglion; **hb**, hindbrain;

in, interneurons; **mb**, midbrain; **mn**, motor neurons; **n**, nodose ganglia, **olf**, olfactory pits; **ot**, otic; **p**, petrosal ganglion; **ph**, pharynx; **s**, stage. Scale bars: (a-f; i-j) 200 μm; (g,h) and (k,l) 100 μm.

Europe PMC Funders Author Manuscripts

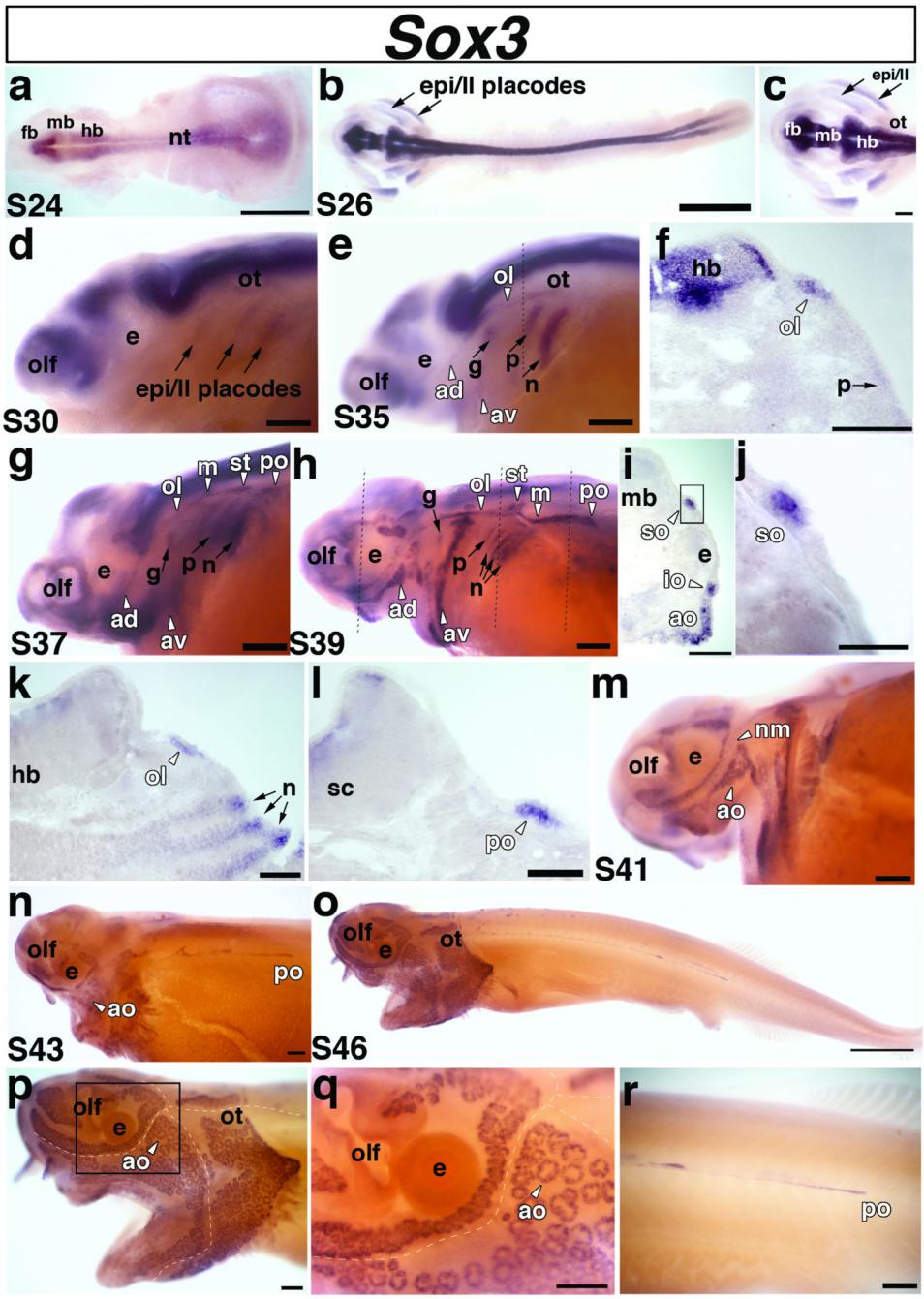

Fig. 6. Paddlefish *Sox3* is expressed in epibranchial and lateral line placodes and sensory organs

Lateral views unless stated otherwise. (**a**) Dorsal view of a stage 24 embryo. *Sox3* is expressed in the neural tube. (**b**) Dorsal view of a stage 26 embryo and **(c)** higher power view of the head region of the stage 26 embryo shown in panel **b**. *Sox3* is expressed in two broad domains representing the presumptive epibranchial and lateral line placodes (arrows) in the pharyngeal arch region. (**d**) Stage 30 embryo. *Sox3* is still present, although faintly, in the lateral regions that comprise the epibranchial and lateral line placodes (epi/ll, arrows). (**e**) Stage 35 embryo. At this stage, *Sox3* can be distinguished in the different epibranchial

placodes: the geniculate (g), petrosal (p), and nodose (n) (arrows), and in the pre-otic lateral line placodes: anterodorsal (av), anteroventral (av), otic lateral line (ol) (arrowheads). The lateral line placodes have begun to elongate and form sensory ridges in the head. *Sox3* is also expressed in the olfactory pits (olf). Dotted line shows plane of section shown in panel **f**. (**f**) A section through the hindbrain (hb) of the embryo shown in panel **e** reveals separate domains of *Sox3* expression in the otic lateral line placode (ol) and faintly in the petrosal placode (p). (**g**) Stage 37 embryo. *Sox3* persists in the epibranchial (arrows) and elongating lateral line (arrowheads) placodes. At this stage, *Sox3* appears to be expressed in all six lateral line placodes: anterodorsal (av), anteroventral (av), otic lateral line (ol), middle (m), supratemporal (st), and posterior (po). (**h**) Stage 39 embryo. *Sox3* expression persists in the elongating lateral line primordia, but the boundaries of individual primordia become difficult to determine owing to the large size of some of the ridges. At this stage, the posterior lateral line placode (po) has begun its extensive migration posteriorly. *Sox3* also continues to be expressed in the epibranchial placodes, although in a weaker, more restricted dorsal region. Dotted lines show planes of sections shown in panels **i-l**. (**i-l**) Sections from different rostrocaudal positions of the stage 39 embryo shown in panel **h**. (**i**) Section through the eye. *Sox3* transcripts are clearly expressed in the developing supraorbital (so) and infraorbital (io) neuromast (mechanosensory) lines. A broad patch of *Sox3* expression can also been seen in a developing field of electrosensory ampullary organs (ao) ventral to the infraorbital (io) canal. (**j**) Higher power view of boxed area in panel **i**, showing *Sox3* transcripts in the supraorbital (so) neuromast canal line. (**k**) Section through the hindbrain. *Sox3* is expressed in the otic lateral line placode (ol) (arrowhead) and in the nodose (n) placodes (arrows). It is also expressed more weakly in “stripes” of cells subjacent to the nodose placodes that may represent pharyngeal pouch endoderm. (**l**) Section through the spinal cord. *Sox3* is seen in the posterior lateral line primordium (po) of the main trunk line. (**m**) Stage 41 embryo. *Sox3* expression is maintained in both mechanosensory neuromasts (nm) and electrosensory ampullary organs (ao), but is no longer seen in the epibranchial placodes. (**n**) Stage 43 embryo. *Sox3* expression is maintained in the developing ampullary organ (ao) fields. The lines of neuromasts in the head are already recessed within lateral line canals and *Sox3* expression is no longer visible in these lines, but can still be seen in the migrating posterior lateral line primordium (po). (**o-r**) Stage 46 embryo. (**o,p**) *Sox3* is maintained in distinct fields of ampullary organs on the head. (**q**) Higher power view of the boxed area in panel **p**. *Sox3* can be seen in individual clusters of ampullary organs. In panels **p** and **q**, the positions of the head neuromast canal lines are indicated by the dotted white lines. (**r**) Higher power view of the migrating *Sox3*-positive posterior lateral line placode (po). Abbreviations: **ad**, anterodorsal lateral line placode; **ao**, ampullary organs (electroreceptors); **av**, anteroventral lateral line placode; **e**, eye; **epi**, epibranchial; **fb**, forebrain; **hb**, hindbrain; **in**, interneurons; **io**, infraorbital neuromast canal; **ll**, lateral line; **m**, middle lateral line placode; **mb**, midbrain; **nm**, neuromasts; **nt**, neural tube; **ol**, otic lateral line placode; **olf**, olfactory pits; **ot**, otic; **po**, posterior lateral line placode of the main trunk; **s**, stage; **so**, supraorbital neuromast canal; **st**, supratemporal lateral line placode. Scale bars: (a,b;o) 1 mm; (c-e; g,h; m,n; p-r); 200 μm (f,i,k) 100 μm; (j,l) 50 μm.

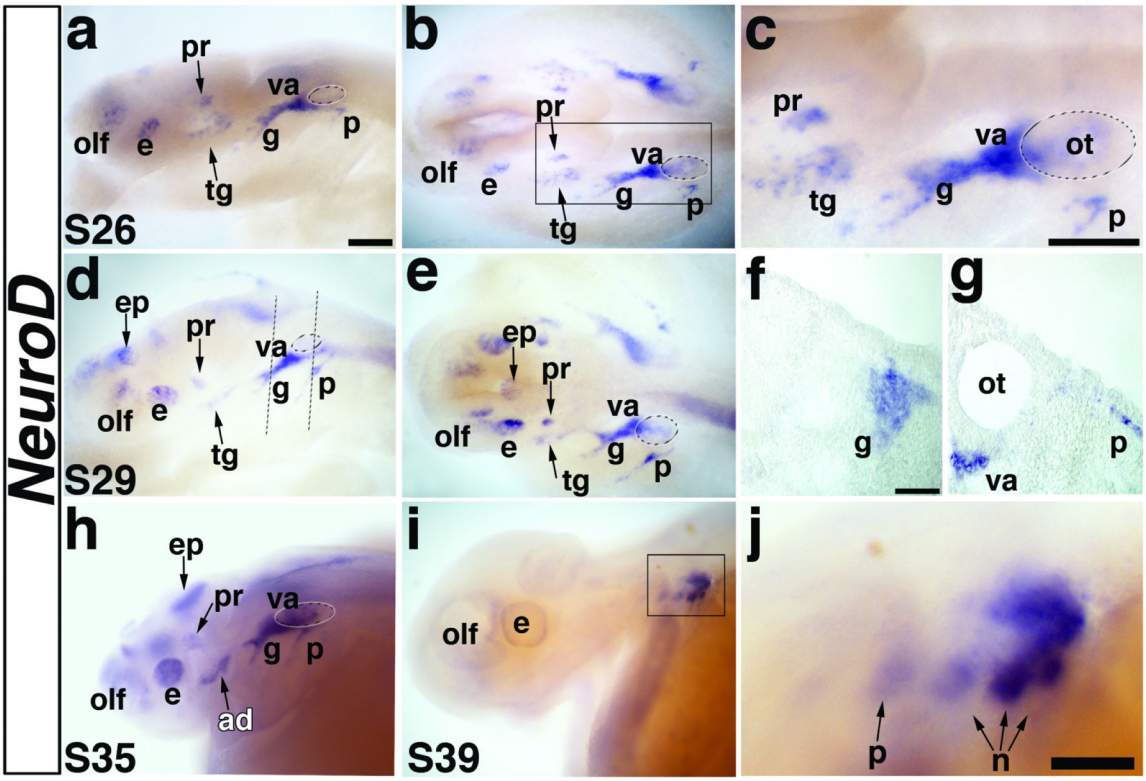

Fig. 7. Paddlefish *NeuroD* is expressed in cranial sensory ganglia

(**a,b**) Lateral and dorsal views, respectively, of a stage 26 embryo showing expression of *NeuroD* in the developing cranial ganglia. (**c**) Higher power view of boxed area in panel **b**. *NeuroD* is expressed in two discrete patches of neuroblasts lateral to the midbrain, i.e., the developing profundal and trigeminal ganglia. *NeuroD* is also expressed in the olfactory placode (olf), in the eye (presumably in differentiating retinal ganglion cells), and in a large domain that includes neuroblasts of the developing geniculate (g) and vestibuloacoustic ganglia (va). The small domain lateral to the otic vesicle is the developing petrosal ganglion. (**d,e**) Lateral and dorsal views of a stage 29 embryo. *NeuroD* expression continues in the previously described domains. It is also seen in the epiphysis (future pineal gland) at this stage. Dotted lines in panel **d** show planes of sections shown in panels **f,g**. (**f**) Section through the developing geniculate ganglion of the stage 29 embryo shown in panels **d,e**, showing *NeuroD* expression in neuroblasts migrating through the mesenchyme. (**g**) Section through the otic vesicle (ot) of the stage 29 embryo shown in panels **d,e**, showing *NeuroD* expression in neuroblasts that have just begun delaminating from the petrosal placode as well as in vestibuloacoustic neuroblasts exiting the otic vesicle. (**h**) Lateral view of a stage 35 embryo. *NeuroD* continues to be expressed in the olfactory pits, eye, epiphysis and weakly in the profundal ganglion. A new domain of expression is observed posterior to the eye, which likely represents neuroblasts of the anterodorsal lateral line ganglion (ad). The large domain of *NeuroD* expression adjacent to the otic vesicle persists, and at this stage, likely also includes lateral line neuroblasts. (**i**) Lateral view of a stage 39 embryo. *NeuroD* expression is completely absent except in the caudalmost epibranchial ganglia. (**j**) Higher power view of the boxed area in i. *NeuroD* is weakly expressed in the petrosal ganglion and

Europe PMC Funders Author Manuscripts

first nodose ganglion, and strongly in the second and third nodose ganglia, demonstrating a rostrocaudal wave of neurogenesis within the epibranchial placode-derived ganglia. Abbreviations: **ad**, anterodorsal lateral line ganglion; **e**, eye; **ep**, epiphysis; **g**, geniculate ganglion, **hb**, hindbrain; **n**, nodose ganglion, **olf**, olfactory pits; **ot**, otic vesicle; **p**, petrosal ganglion, **pr**, profundal ganglion; **s**, stage, **tr**, trigeminal ganglion, **va**, vestibuloacoustic ganglion. Scale bars: (a-e; h,i) 200 μm; (f,g) 50 μm; (j) 100 μm.

Europe PMC Funders Author Manuscripts